Carboxylic Acid- and Ester-Functionalized Siloxane Scaffolds on Glass Studied by Broadband Sum Frequency Generation

Andrea B. Voges, Hind A. Al-Abadleh, Michael J. Musorrafiti, Paul A. Bertin, SonBinh T. Nguyen, and Franz M. Geiger*

Department of Chemistry, Northwestern University, 2145 Sheridan Road, Evanston, Illinois 60208-3113

Received: July 31, 2004; In Final Form: September 15, 2004

Broadband sum frequency generation has been used to characterize glass surfaces functionalized with siloxanes containing terminal carboxylic acid and ester functional groups. ω-Ester silanes can be used in the preparations of ester-functionalized glass surfaces, which yield acid-functionalized surfaces via hydrolysis. This general methodology can be used in environmental, biochemical, or materials science surface chemistry to generate surfaces with tunable physical and chemical properties. Definitive characterization of these carboxylate-functionalized glass surfaces can be performed in the C−H vibrational frequency region using sum frequency generation.

I. Introduction

The functionalization of silica surfaces using siloxane chemistry has received much attention as this process allows for the convenient generation of transparent substrates with tailored surface properties. Similar to thiol-functionalized gold substrates, appropriately functionalized siloxanes on silica substrates can be used as linker scaffolds for a wide variety of organic and inorganic compounds that are important in environmental chemistry, materials science, biological systems and industrial applications.[1−10] In this paper, we focus on the application of siloxanes that are terminated with carboxylic acid and ester functional groups to glass substrates, thereby extending the scope of sum frequency generation (SFG) work on functionalized silica surfaces, which, until now, had been limited to pure hydrocarbon systems. Functionalized siloxane scaffolds can be used for the construction of complex surfaces and interfaces with high chemical stability and tunable chemical and physical properties. Likewise, these scaffolds can be used for studying environmentally important heterogeneous systems where carboxylic acid and ester functional groups are common.

Our work utilizes broadband sum frequency generation (BBSFG) to characterize three types of adlayers on glass. The organic adlayers were chosen to contain, specifically, an acid-terminated alkyl chain, several ester-functionalized alkyl chains, and a nonfunctionalized alkyl chain. The last system was studied to provide a comparison with existing SFG studies on silanized surfaces. The ester adlayers were chosen to verify spectral peaks observed in the experiments and to demonstrate the capability of SFG to distinguish between various ester functional groups. They also serve as precursors to the acid-functionalized surface.

Nonlinear optical spectroscopy has been applied to characterize aliphatic carbon chains chemically bound to silica and silicon substrates. IR−vis SFG is an appropriate tool for studying such interfaces, as it yields infrared spectra that are inherently surface and interface specific.[11,12] SFG spectra of simple siloxane-modified surfaces were recorded and analyzed by several groups. Using SFG, Shen studied octadecyltrichlorosilane (OTS) at the silica/air interface and reported the CH_3 symmetric stretch at 2878 cm^{-1}, the CH_3 asymmetric stretch at 2964 cm^{-1}, and the CH_3 Fermi resonance at 2942 cm^{-1}.[13] However, CH_2 contributions were not found. Liu et al. focused on the adsorption of OTS to silica/solvent interfaces, paying special attention to the role that trace amounts of water play in the cross-linking chemistry occurring at the interface.[14] These workers assigned the CH_3 Fermi resonance to occur at 2946 cm^{-1}, the CH_3 symmetric stretch at 2878 cm^{-1}, and the CH_2 symmetric stretch at 2850 cm^{-1}. This last peak disappears as the number density of gauche defects decreases with increasing order within the siloxane adlayer. Recently, Chen et al. reported SFG spectra of bulk liquid silane/polymer interfaces.[15] They designated the CH_2 symmetric and asymmetric stretches of OTS to occur at 2850 and 2930 cm^{-1}, respectively, and the silane CH_3 symmetric stretch at 2870 cm^{-1}. Similar peak assignments for C_{18} carbon chains chemically bound to Si(111) wafers in air were given by Nihonyanagi et al.[16] Lagutchev et al. studied OTS and C_8 carbon chains on silica, and reported, for both adlayers, the CH_3 symmetric stretch at 2875 cm^{-1} and the CH_3 Fermi resonance at 2940 cm^{-1}, whereas only the shorter carbon chain showed the CH_2 symmetric stretch at 2846 cm^{-1} and the CH_2 asymmetric stretch at 2920 cm^{-1}.

In general, the SFG peak assignments for alkyl-chain-functionalized silica and silicon substrates are in good agreement with the ones obtained from linear IR spectroscopy for siloxanes on glass and long chain aliphatic compounds.[17−19] They provide the basis for our present work, which is focused on the characterization of acid- and ester-functionalized siloxane scaffolds on glass using BBSFG. The characterization of these scaffolds is necessary in order to generate more complex surfaces, which can be designed with high control over molecular orientation, surface order and disorder, and chemical function.

II. Experimental Section

A. Broadband Sum Frequency Generation. Detailed descriptions of theoretical and experimental aspects of sum frequency generation (SFG) can be found elsewhere;[12,13,20−25] hence, the following section is intended to serve only as a brief

* Author to whom correspondence should be addressed. E-mail: geigerf@chem.northwestern.edu.

10.1021/jp046564x CCC: $27.50
Published on Web 11/10/2004

overview. If the incoming electric fields are of sufficient intensity, coupling of an IR pulse with a visible pump pulse in a noncentrosymmetric medium, such as an interface, will lead to an SFG signal.[13] The signal is inherently specific to the noncentrosymmetric environment and therefore yields information from the surface without contributions from the bulk phases above and below the interface.[26] Resonance-enhanced SFG can be used in the IR frequency region to probe vibrational modes of interfaces and their adsorbates, lending molecular specificity to this intrinsically surface selective technique.

The intensity of the SFG signal, I_{SFG}, is directly proportional to the square modulus of the second-order susceptibility of the interface, $\chi^{(2)}$, and the intensity of the input visible and IR electric fields, I_{Vis} and I_{IR} respectively, as shown in eq 1[27]

$$I_{SFG} \propto |\chi^{(2)}|^2 I_{Vis} I_{IR} \tag{1}$$

The nonlinear susceptibility $\chi^{(2)}$ can be broken down into a nonresonant contribution and a resonant contribution, $\chi_{NR}^{(2)}$ and $\chi_{R\nu}^{(2)}$, respectively (eq 2).[27]

$$I_{SFG} \propto |\chi_{NR}^{(2)} + \sum_{\nu=1}^{n} \chi_{R\nu}^{(2)} e^{i\gamma_\nu}|^2 \tag{2}$$

In this expression, $\chi_{R\nu}^{(2)}$ contains resonant contributions from each vibrational mode, ν, and the contributions from the n vibrational modes are coupled by their relative phases, γ_ν. The resonant contribution to the second-order susceptibility is proportional to the number of molecules, N_{ads}, and the molecular hyperpolarizability, β_ν, averaged over all orientations of molecules at the surface (eq 3).[21]

$$\chi_{R\nu}^{(2)} \propto N_{ads} \langle \beta_\nu \rangle \tag{3}$$

The value of β_ν increases when the frequency of the incoming IR beam matches a vibrational transition of the adsorbate or interface, according to eq 4[24]

$$\beta_\nu \propto \frac{A_{\nu,ij} M_{\nu,k}}{\omega_{IR} - \omega_\nu + i\Gamma_\nu} \tag{4}$$

For a given mode ν, A_ν is the Raman transition probability, M_ν is the IR transition dipole moment, i, j, and k refer to the surface coordinate system, ω_ν is the IR frequency of the vibrational mode in the surface-bound species, ω_{IR} is the frequency of the IR probe light, and Γ_ν is the damping coefficient that avoids singularities in eq 4 and can be used to describe the natural line width of the IR resonance. Equation 4 shows that observable modes have to be IR and Raman active. Enhancement of β_ν leads to resonant enhancement of $\chi_{R\nu}^{(2)}$ and thus of the SFG signal intensity. For hydrocarbons on insulator surfaces, the nonresonant contributions to the SFG signal are small in general.[28]

The complete vibrational spectrum for an interface and its adsorbates can be acquired by scanning the frequency of the incoming IR beam. This allows for the spectroscopic characterization of the interface. In contrast to such scanning techniques, IR fields that are broad in the frequency domain, such as those produced by femtosecond IR systems, allow for the collection of SFG spectra within a single laser pulse. The spectral resolution is chiefly determined by the bandwidth of the visible pump pulse[25,29] and, to a smaller extent, the monochromator and detector resolutions. Broadband sum frequency generation (BBSFG), as pioneered by Richter et al.,[25] can lead to shorter collection times compared to scanning SFG experiments as a step toward real time monitoring of in situ reactions and dynamics.[25,29]

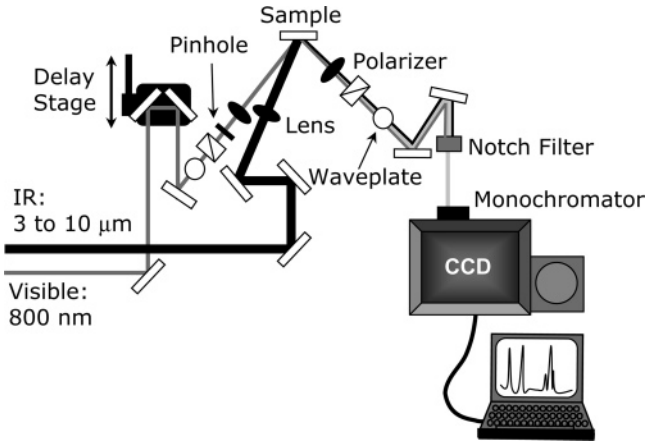

Figure 1. Experimental layout of the BBSFG system.

B. Laser and Detection System. The BBSFG studies are carried out using an 800-nm 120-fs regeneratively amplified Ti:sapphire system (Hurricane, Spectra Physics), operating at a kilohertz repetition rate. The Hurricane system pumps an optical parametric amplifier (OPA-800CF, Spectra Physics) containing a β-barium borate (BBO) crystal for signal and idler generation and an $AgGaS_2$ crystal (cut for 4 μm) for difference frequency generation. The BBO crystal generates a signal beam between 1.1 and 1.6 μm and an idler beam between 1.6 and 2.6 μm that are mixed in the difference frequency generation crystal to produce infrared radiation between 3 and 10 μm. Figure 1 illustrates the layout of the BBSFG system. The visible pump beam from the regenerative amplifier is filtered with two narrow band-pass filters (F1.1-800.0-UNBLK-1.00, CVI) to provide an 800-nm pump pulse with a bandwidth of 1.57 nm. A time delay stage and an achromatic waveplate (MWPAA2-12-400-700, Karl Lambrecht Corp.) in the visible input line allow for the delay and polarization rotation of the visible pulse, respectively. Typical visible pulse energies range around 40 μJ; infrared pulse energies range between 10 and 20 μJ. The IR light field is focused onto the sample by a 25-mm diameter BaF_2 lens with a 200-mm focal length (BF-PX-25-200, ISP Optics) at an angle approximately 60° from normal to the substrate surface. The visible light field is focused onto the sample by a 25-mm diameter BK-7/SF5 glass lens with a 150-mm focal length (J32-494, Edmund Scientific) at an angle approximately 45° from normal to the substrate surface.

For the studies on the functionalized surfaces presented herein, the broadband IR output from the optical parametric amplifier is tuned to a center frequency near 2900 cm^{-1} with a bandwidth of ~140 cm^{-1}. The IR bandwidth was measured indirectly by collecting the BBSFG spectrum of a thin gold film (Figure 2). Specific polarization states of the coherently scattered SFG signal from the sample are selected by a polarizer−analyzer (Glan Laser Polarizer GL10, Nova Phase Inc.), after which the SFG signal is spatially filtered with a pinhole and optically filtered using an 800-nm notch filter (Notch Plus Filter, Kaiser Optical Systems, Inc.) to remove the scattered fundamental pump light. After polarization selection and prior to detection, the SFG signal is passed through a waveplate (MWPAA2-12-400-700, Karl Lambrecht Corp.) to rotate its polarization for optimal throughput in a 0.5-m spectrograph (Acton Research, 1200 grooves/mm grating on turret). Detection of the dispersed signal is carried out with a liquid-nitrogen-cooled, back-thinned charged coupled device (CCD) camera (Roper Scientific, 1340 × 100 pixels) operating at −110 °C that allows spectra to be

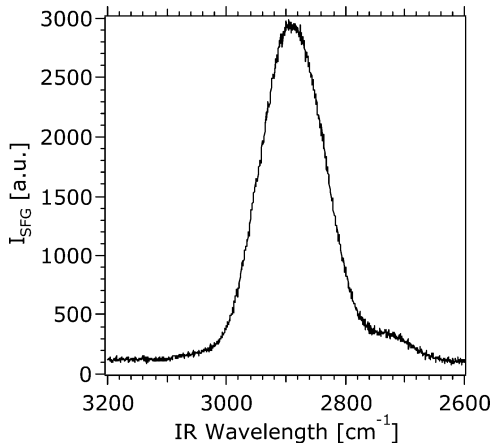

Figure 2. A BBSFG spectrum taken of a gold film deposited on a glass slide.

collected with a time resolution of up to 1 ms. The spectra of the functionalized substrates shown in this work were collected in the ssp polarization combination (i.e., by detecting the s-polarized component of the SFG signal while sending s-polarized visible and p-polarized IR input beams onto the sample). The SFG experiments were carried out by probing the surface from the air side (i.e., without using a total internal reflection geometry).

C. Spectroscopic Calibration, Signal-to-Noise, and Data Acquisition Time. To overcome the challenges associated with BBSFG spectroscopy of transparent insulating substrates with negligible nonresonant contributions to the SFG signal, a step-by-step experimental approach was taken. First, the BBSFG spectrum of the gold samples prepared as described above was recorded. We started with gold because this metal surface has high nonresonant contributions to the SFG signal, which make them optimal for initial alignment. Then, the BBSFG spectrum of octadecanethiol (ODT) on gold was taken in order to optimize alignment and signal delivery. Subsequently, the BBSFG spectra of dimethyl sulfoxide (DMSO) and of poly(methyl methacrylate) (PMMA) on glass were recorded. This allowed for the optimization of the BBSFG setup for transparent substrates and provided a spectral calibration standard. Further, the relatively strong SFG signals from these samples enabled us to improve the signal-to-noise ratio using binning and signal averaging techniques and to assess the spectral resolution of the experiment. Finally, the BBSFG spectra of various functionalized siloxanes on glass were recorded.

The nonresonant BBSFG spectrum of gold films prepared as discussed in the following section is shown in Figure 2 and found to be independent of gold film thickness. The BBSFG spectrum of ODT on gold, recorded within 200 ms (Figure 3), agrees well with the original BBSFG spectrum of ODT published by Richter et al.[25] Figure 3 also shows that as the 800-nm pump pulse is delayed with respect to the broadband infrared pulse the BBSFG peak positions do not change significantly and have a standard deviation of around 3 cm^{-1} (the peak positions for the two peaks labeled a and b in Figure 3, namely, the CH_3 symmetric stretch and the CH_3 Fermi resonance, were examined here).

Figure 4 shows the methyl symmetric stretch of DMSO on glass. This spectrum was collected using a data acquisition time of 200 ms. A fit of eq 4 to the spectrum results in a bandwidth of 18 cm^{-1}, which agrees well with the one reported by Allen et al.,[30] indicating a spectral resolution of at least 18 cm^{-1} for our experimental setup.

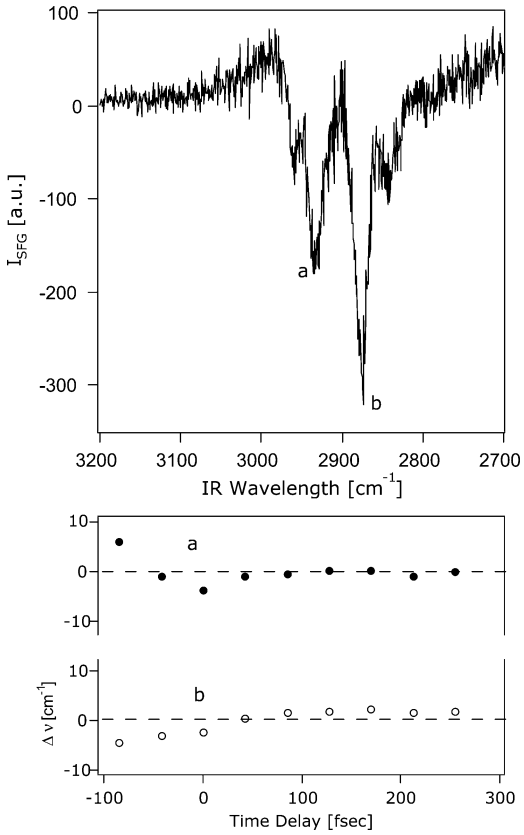

Figure 3. (Top) A BBSFG spectrum taken of octadecanethiol on a gold film deposited on a glass slide recorded within 200 ms. (Bottom) Frequency change of peaks a and b as a function of time delay between the visible pump pulse and the broadband infrared pulse.

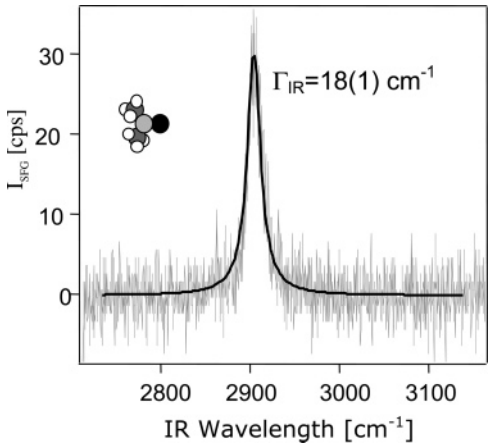

Figure 4. BBSFG spectrum of DMSO on a glass slide, taken with an acquisition time of 200 ms. The fit (black line) of eq 4 to the data indicates a bandwidth of ~18 cm^{-1}.

The spectrograph is calibrated to the 2955 cm^{-1} peak from the symmetric stretch of the ester methyl group reported for PMMA using SFG spectroscopy.[15,31,32] The reproducibility of the absolute SFG peak position is ± 5 cm^{-1}. Reproducibility was determined by comparing several SFG spectra of the same PMMA sample that were taken in series, with the substrate removed from the sample stage and repositioned onto the sample stage between each spectral acquisition. To reduce the noise in the data, 20 spectra were taken sequentially and signal averaged for a given sample, each with their own individual background. The enhancement in the signal-to-noise ratio is shown in Figure 5 for PMMA. Except when noted, spectra of functionalized substrates shown are the result of averaging three independently

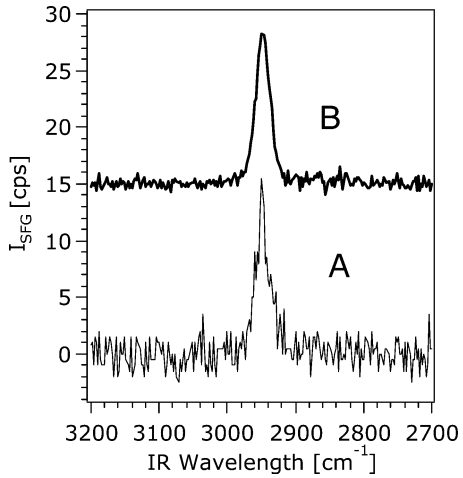

Figure 5. (A) One unaveraged PMMA spectrum recorded within 10 s. (B) The average of 20 BBSFG spectra, each recorded within 10 s, of PMMA (offset by 15 cps for clarity). The polarization combination is ssp.

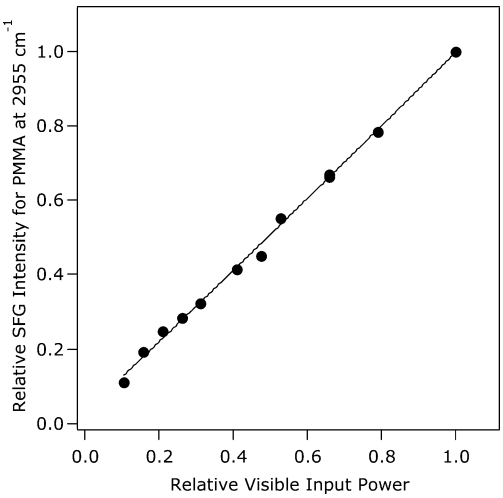

Figure 6. Relative SFG signal intensity of the 2955 cm^{-1} peak of PMMA as a function of relative visible input power at 800 nm.

collected data sets, each containing 20 background-subtracted spectra. This procedure ensured the reproducibility of the spectral features recorded.

To lower the susceptibility of the CCD chip to cosmic rays and to further lower the background scatter detected by the CCD chip, data was only collected from a strip of pixels 20 rows tall along the center long axis of the chip. During the collection of an individual spectrum, the raw signal is horizontally binned across three pixels. Because the resolution of the spectrograph is 1.1 cm^{-1} per pixel and the spectral resolution of the experiments is $\sim$20 cm^{-1}, on-line horizontal binning of the collected data does not diminish the resolution of the experiment but significantly enhances the signal intensity.

Energy-dependence studies were carried out using a glass slide spin-coated with 1 wt % PMMA in toluene to ensure that the intensity of the SFG signal was linearly dependent on the visible pump energy, as expected from eq 1. Figure 6 shows that this is the case. SFG signal intensities are found to follow a one-to-one correlation with the incident pump energy, which is consistent with eq 1. Departure from this one-to-one correlation is observed for visible pump energies above 100 μJ.

D. Synthesis and Substrate Preparation. *General Considerations and Materials.* All synthetic manipulations were performed under dry nitrogen using either standard Schlenk techniques or an inert-atmosphere glovebox. 2-Propanol was distilled over $Mg(O^iPr)_2$ and saturated with nitrogen prior to use, and triethylamine was distilled over calcium hydride and saturated with nitrogen prior to use. All other solvents were dried and purified using the Dow−Grubbs solvent system[33] under argon and saturated with argon before use. Octyltrichlorosilane was distilled under vacuum and stored in an inert-atmosphere glovebox. Trichlorosilane was distilled over quinoline and vacuum transferred into an airtight solvent bulb, followed by transfer to an inert-atmosphere glovebox. Except for the deuterated solvents (Cambridge Isotope Laboratories), 10-undecylenic acid (Acros Organics), and chloroplatinic acid (Strem Chemicals, Inc), all reagents were purchased from Aldrich and used without further purification, unless otherwise noted.

Organotrichlorosilanes. The methyl ester-terminated trichlorosilane (11-(trichlorosilyl)undecanoic acid methyl ester) and the fluorinated ethyl ester-terminated trichlorosilane (11-(trichlorosilyl)undecanoic acid 2,2,2-trifluoroethyl ester) were prepared following literature procedure.[34] The synthesis of the deuterated methyl ester-terminated trichlorosilane (11-(trichlorosilyl)undecanoic acid methyl-d_3 ester) has been described elsewhere.[35] The synthesis of the isopropyl ester-terminated trichlorosilane (11-(trichlorosilyl)undecanoic acid isopropyl ester) is described in detail below.

Instrumentation. ^1H and ^{13}C NMR spectra were recorded on a Varian INOVA 500 FT-NMR spectrometer (499.6 MHz for ^1H NMR, 125.6 MHz for ^{13}C NMR). ^1H NMR data are reported as follows: chemical shift (multiplicity (b = broad, s = singlet, d = doublet, t = triplet, q = quartet, and m = multiplet), integration, and peak assignments). ^1H and ^{13}C chemical shifts are reported in ppm downfield from tetramethylsilane (TMS). High-resolution atmospheric pressure chemical ionization mass spectrometric data (HRMS-APCI) was obtained on a Finnigan LCQ Advantage instrument.

Synthesis of Isopropyl Undecenylate (Undecenoic Acid Isopropyl Ester). Into a 50-mL Schlenk flask was added 10-undecylenic acid (1.95 g, 10.6 mmol). The flask was placed under nitrogen, and dry CH_2Cl_2 (15 mL) was added via cannula, followed by oxalyl chloride (16 mL of a 2 M solution in CH_2Cl_2, 32 mmol). The solution was stirred for 2 h at room temperature. The solvent and excess oxalyl chloride were removed under vacuum, and the resulting acid chloride was redissolved in dry CH_2Cl_2 (15 mL).

Into a separate 50-mL Schlenk flask was added 2-propanol (4 mL, 52 mmol) under nitrogen. CH_2Cl_2 (10 mL) was added, followed by triethylamine (4 mL, 33 mmol). This flask was fitted with a pressure-equalizing dropping funnel. The acid chloride solution from the first flask was transferred to the dropping funnel via cannula and subsequently added dropwise to the stirring solution below over a period of 10 min. The dropping funnel was replaced with a reflux condenser and the mixture was stirred at 75 °C for an additional 2 h. Excess 2-propanol and triethylamine were removed under vacuum, and the contents were transferred to a 250-mL separatory funnel with ether (100 mL). The organic layer was washed with water (2 × 50 mL) and brine (50 mL), dried over sodium sulfate, and filtered. The solvent was removed under reduced pressure, and the product was vacuum distilled to give a pure (>99%, GC analysis) colorless liquid (2.03 g, 9.00 mmol, 85%). ^1H NMR ($CDCl_3$): δ 1.23 (d, 6H, J = 6.5 Hz, isopropyl-CH_3), 1.29−1.37 (m, 10H, alkyl-CH_2), 1.60−1.62 (m, 2H, COCH$_2$CH_2), 2.04 (dt, 2H, J = 7.5 and 7.0 Hz, CH$_2$=CHCH_2), 2.26 (t, 2H, J = 7.5 Hz, COCH_2), 4.92−5.00 (m, 2H, CH_2=CH), 5.02 (m,

1H, isopropyl-C*H*), 5.82 (ddt, 1H, $J = 17.0$, 10.5, and 7.0 Hz, CH_2═C*H*). ^{13}C NMR ($CDCl_3$): δ 21.7, 22.1, 25.3, 29.1−29.5 (m, 5C), 34.0, 34.9, 67.5, 114.4, 139.4, 173.7. HRMS-APCI calcd. for $C_{14}H_{27}O_2$: 227.2006. Found: 227.2004.

Synthesis of 11-(Trichlorosilyl)-undecanoic Acid Isopropyl Ester. Isopropyl undecenylate (1.00 g, 4.4 mmol), trichlorosilane (2 mL, 20 mmol), and 20 μL of a 4% solution of chloroplatinic acid in 2-propanol were combined in a 25-mL Schlenk flask. The mixture was stirred at room temperature for 18 h. The progress of the reaction was monitored by the disappearance of olefinic protons by ^{1}H NMR. Upon completion, excess trichlorosilane was removed under reduced pressure, and the product was isolated by vacuum distillation to give a colorless liquid (1.50 g, 4.1 mmol, 94%). ^{1}H NMR ($CDCl_3$): δ 1.21 (d, 6H, $J = 6.5$ Hz, isopropyl-CH_3), 1.27−1.40 (m, 16H, alkyl-CH_2), 1.57 (m, 2H, $COCH_2CH_2$), 2.24 (t, 2H, $J = 7.5$ Hz, $COCH_2$), 4.99 (m, 1H, isopropyl-C*H*). ^{13}C NMR ($CDCl_3$): δ 21.7, 22.0, 22.4, 24.5, 25.2, 29.1, 29.3, 29.4 (m, 2C), 29.5, 32.0, 34.9, 67.5, 173.5. HRMS-APCI calcd. for $C_{14}H_{28}O_2Cl_2{}^{37}ClSi$: 363.0889. Found: 363.0883.

Preparation of Functionalized Glass Surfaces. Glass slides were cleaned in a N_2-filled inert-atmosphere glovebox using one of two different techniques. The slides were cleaned by soaking either in (1) H_2SO_4 for 2 h or (2) boiling piranha solution (3:1, concentrated H_2SO_4 to 30% H_2O_2) for 1 h. *CAUTION: working with piranha solution is highly dangerous and should only be done after reading and understanding the appropriate MSDS sheets*. Slides were also cleaned using a plasma cleaner chamber (Harrick) operated in air at high power for 15 min. The three sample preparation and cleaning procedures yielded comparable and reproducible BBSFG spectra.

After substrate preparation, the clean substrates were transferred to a N_2-filled inert-atmosphere glovebox and exposed to a 1% (v/v) solution of the desired organotrichlorosilane in dry toluene for 1 h. The solution was decanted, and the surface was rinsed with excess toluene and placed in an oven at 110 °C for 1 h. The carboxylic acid-functionalized surfaces were generated by immersing the ester-functionalized surfaces in 2.4 M HCl (aq) at 85 °C for 2 h. Upon being cooled to room temperature, the substrates were rinsed with excess water and stored in a drybox, except for the carboxylic acid-functionalized substrate, which was stored under water prior to analysis. The surfaces were characterized by static contact angle measurements and BBSFG measurements. Contact angle measurements show static contact angles of 65° for the methyl ester siloxanes before hydrolysis and 47° after hydrolysis, consistent with an increase in hydrophilicity of the siloxane following hydrolysis of the ester.[36,37]

Gold Substrates. The gold film was prepared by thermal evaporation of 10−15 nm of Ti (99.99%; Alfa Aesar; Ward Hill, MA) on a glass slide followed by 60−120 nm of Au (99.99% Alfa Aesar; Ward Hill, MA). This was accomplished using an Edwards Auto306 Turbo Evaporator equipped with a turbopump and an Edwards FTM6 quartz crystal microbalance to determine film thickness. Au and Ti depositions were conducted at room temperature at a rate of 1 nm/s and a base pressure of 8×10^{-8} Torr. Signal detection is carried out as described previously.

III. Results and Discussion

Figure 7 shows the ssp spectrum of a glass surface functionalized with $Cl_3Si(CH_2)_7CH_3$ (Figure 7A) and $Cl_3Si(CH_2)_{10}COOCH_3$ (Figure 7B). The BBSFG spectrum of the ester-functionalized siloxane after hydrolysis is shown as well (Figure 7C). Table 1 contains a summary of peak positions as they appear on the BBSFG spectra.

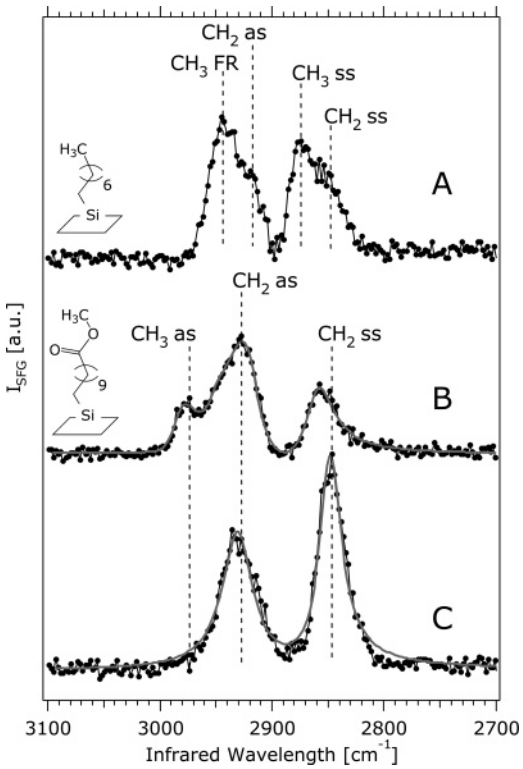

Figure 7. BBSFG spectra of an alkyl-functionalized glass substrate (A) and of a methyl ester-functionalized glass substrate before (B) and after (C) hydrolysis. Spectra offset for clarity. The polarization combination is ssp. Fits of eqs 2 and 4 to the spectra are shown as well.

The alkyl-functionalized surface (Figure 7A) shows a peak at 2945 cm^{-1}, which is assigned to the Fermi resonance of the CH_3 symmetric stretch with a CH_3 bending overtone,[20,38,39] and a peak at 2875 cm^{-1}, which is assigned to the CH_3 symmetric stretch.[20,40,41] In general, adjacent methylene groups in long chain aliphatic molecules at interfaces are often found to be nearly centrosymmetric, resulting in very small contributions to the SFG spectrum between 2800 and 3000 cm^{-1} in the ssp polarization combination.[42] Therefore, it is reasonable to expect strong spectral contributions from the terminal methyl group of the siloxane adlayers and small contributions from the methylene groups. If the alkyl chains were distorted, the resulting asymmetry would lead to spectral contributions of methylene groups to the SFG spectra. Such distortion has been observed previously and can be attributed to the presence of trans−gauche defects along the length of the chain,[41,43,44] with defect site densities depending on surface coverage and solvent water content.[14] The shoulders at 2919 and 2854 cm^{-1} are therefore assigned to the CH_2 asymmetric and symmetric stretches, respectively, with possible contributions from a CH_2 Fermi resonance.[21,25,28,45] The CH_2 Fermi resonance is in phase with the CH_2 symmetric stretch and can thus broaden the higher energy feature.[28] In general, strong signal intensities from CH_2 groups indicate significant disruption in the ordered packing of the siloxane scaffolds, suggesting a high degree of chain, or gauche, defects.

The spectrum of the ester-functionalized surface (Figure 7B) is found to be significantly different than that of the alkyl-functionalized adlayer. Here, the CH_3 asymmetric peak is observed near 2975 cm^{-1}, which is consistent with the CH_3 asymmetric stretch frequency of methanol and polymers con-

TABLE 1: Summary of CH_2 and CH_3 Stretches Recorded for the Functionalized Substrates under Investigation in This Work[a]

Peak Assignments for Scaffolds [cm^{-1}]		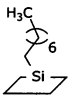	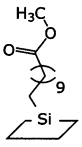	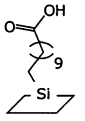	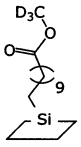	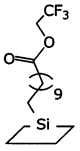	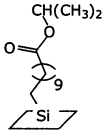
CH_2	as	2919	2927	2931	2924	2928	-
	ss	2854	2857	2847	2851	2861	2852
CH_3	as	-	2975	-	-	-	2950
	ss	2875	-	-	-	-	2880
	FR	2945	-	-	-	-	2934

[a] Polarization: ssp.

taining methoxy groups.[38,46,47] The peak at 2927 cm^{-1} is assigned to the CH_2 asymmetric stretch with possible contributions from the Fermi resonance of the terminal methyl group around 2940 cm^{-1}. The peak at 2857 cm^{-1} is indicative of the CH_2 symmetric stretch and is only shifted slightly from the alkane SFG spectrum. To quantitatively analyze the spectrum, a specially written function consisting of four Lorentzian functions with individual phases referenced to the phase of the lowest energy vibrational mode and with a nonresonant phase of zero was fit to the ester-functionalized surface (Figure 7B). The function was fit to the data using Igor Pro software. The frequencies and their peak assignments are as follows: 2861(1) cm^{-1} for the CH_2 symmetric stretch, 2920(1) cm^{-1} for the CH_2 asymmetric stretch, 2953(4) cm^{-1} for the Fermi resonance or symmetric stretch of the terminal methyl group, and 2983(2) cm^{-1} for the asymmetric stretch of the terminal methyl group. These frequencies are in good agreement with the ones obtained from visual inspection of the BBSFG spectrum.

The strong signal contributions from the methylene stretches in the ester-functionalized siloxane are striking. These signal contributions can originate from gauche defects along the carbon chain,[41,42] or from the methylene group adjacent to the carboxyl group, which is expected to break the local symmetry around the neighboring methylene group even in an all-trans configured carbon chain. Lagutchev et al. applied SFG and X-ray photoelectron spectrosopy to fluorinated alkylsiloxanes on fused silica and interpreted this effect in the context of charge redistribution.[44] In the siloxane-modified surfaces investigated in the present study, the ester moiety breaks the inversion symmetry of the α and β CH_2 groups. This symmetry breaking could result in significant contributions of the α and β CH_2 groups to the SFG spectrum as compared to the contributions of CH_2 groups that are farther away from the carboxyl group.

After complete acid hydrolysis of the methyl ester-terminated substrate, we would expect to see contributions only from the CH_2 groups along the carbon chain of the $-Si(CH_2)_{10}COOH$ molecules. The SFG spectrum obtained following ester hydrolysis is consistent with such expectations and gives direct evidence that the hydrolysis of the surface-bound methyl ester siloxane has occurred (Figure 7C). The BBSFG spectrum of the interface after hydrolysis lacks the 2975 cm^{-1} CH_3 peak of the methoxy group seen in the spectrum before hydrolysis. The remaining two peaks at 2931 and 2847 cm^{-1} are assigned to the CH_2 asymmetric and symmetric stretches, respectively. The higher energy spectral feature may also include the CH_2 Fermi resonance. Similar to the methyl ester-functionalized siloxane, the spectral signatures of the CH_2 groups can be attributed in part to gauche defects along the carbon chain or to the disruption of the inversion symmetry of methylene groups adjacent to the highly polar carboxyl end group or both. To quantitatively analyze the spectrum, two functions were fit to the SFG spectrum obtained following ester hydrolysis (Figure 7C). A fit expression consisting of two Lorentzian functions resulted in the following frequencies, listed together with their peak assignments: 2849(1) cm^{-1} for the CH_2 symmetric stretch and 2930(1) cm^{-1} for the CH_2 asymmetric stretch. A second fit attempt using three Lorentzian functions to test for the presence of a shoulder at 2953 cm^{-1}, which may be residual from the Fermi resonance or symmetric stretch of the terminal methyl group and is seen in the ester, resulted in the following frequencies: 2848(6), 2883(5), and 2936(4) cm^{-1}. Clearly, the fit with three vibrational modes converged away from physically meaningful initial input parameters.

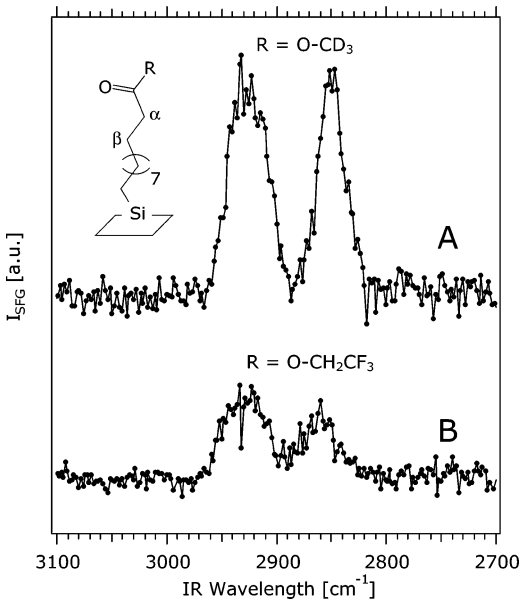

Figure 8. BBSFG spectra of a glass substrate functionalized with a CD_3-deuterated methyl ester siloxane (A) and with a fluorinated ester siloxane (B). Spectra offset for clarity. The polarization combination is ssp.

These spectral assignments are confirmed by BBSFG spectra taken of two ester-functionalized siloxanes, namely, $-Si(CH_2)_{10}COOCD_3$, and $-Si(CH_2)_{10}COOCH_2CF_3$ (Figure 8). Replacement of the CH_3 groups with CD_3 or CH_2CF_3 groups in the methyl ester scaffolds deconvolutes the CH_3 and CH_2 stretches of the methyl ester-functionalized siloxane and yields spectra comparable to that of the hydrolyzed methyl ester. The BBSFG peaks for the CD_3 ester (Figure 8A) and the CH_2CF_3 terminated ester (Figure 8B) are assigned to the asymmetric and symmetric CH_2 stretches (2924 and 2851 cm^{-1} for the CD_3 ester,

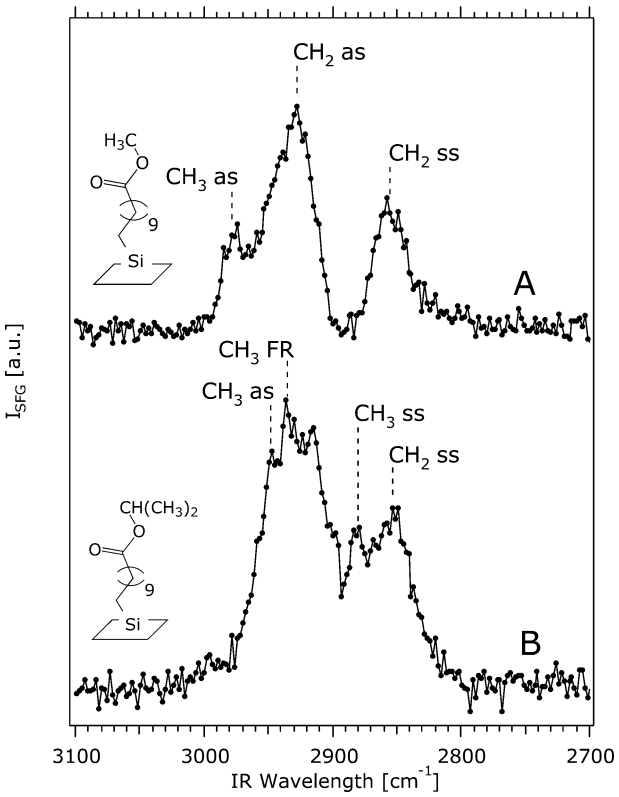

Figure 9. BBSFG spectra of a glass substrate functionalized with a methyl ester-terminated siloxane (A) and with an isopropyl ester-terminated siloxane (B). Spectra offset for clarity. The polarization combination is ssp.

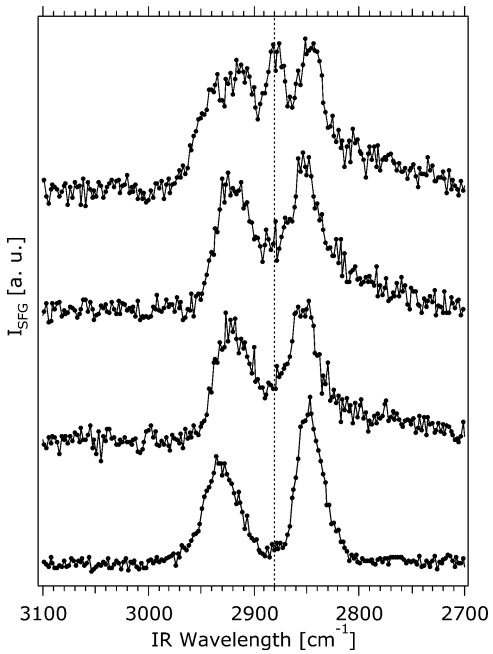

Figure 10. BBSFG spectra of a glass substrate functionalized with a carboxylic acid-terminated siloxane shown before rinsing with benzene (top), after two successive rinses with benzene, and after a number of benzene rinses (bottom) that resulted in identical spectra. Spectra offset for clarity.

respectively; 2928 and 2861 cm^{-1} for the CH_2CF_3 ester, respectively). Future experiments will focus on tuning the BBSFG spectrometer to the C−D stretching region and building a total internal reflection setup in order to gain further spectroscopic information about the hydrolysis reaction and the structure of the surface bound species in this spectroscopic region.

The sensitivity of BBSFG allows for differentiation between surfaces functionalized with various ester siloxanes. Figure 9 shows the BBSFG spectrum of a methyl ester-terminated siloxane on glass (Figure 9A) in comparison with that of an isopropyl ester-terminated siloxane on glass, $-Si(CH_2)_{10}$-$COOCH(CH_3)_2$ (Figure 9B). The isopropyl ester-terminated scaffold shows both the asymmetric and the symmetric CH_3 stretches, assigned to the shoulder at 2950 cm^{-1} and the peak at 2880 cm^{-1}, respectively. The peak at 2915 cm^{-1} could be due to the CH_2 Fermi resonance or the asymmetric stretch of the CH_2 groups whereas the peak at 2852 cm^{-1} is attributed to CH_2 symmetric stretches. The feature at 2934 cm^{-1} is assigned to the Fermi resonance of the CH_3 symmetric stretch with a CH_3 bending overtone. BBSFG spectra of the isopropyl ester-terminated siloxane-modified surfaces are reproducible and distinct from those of the methyl ester-terminated siloxane-modified surfaces. As there are no signal contributions above 3000 cm^{-1}, the methine stretch is not observed. A summary of the peak assignments presented in this work is provided in Table 1.

Proper cleaning of the substrates is found to be critical for accurate identification of surface species. Immediately before use, the siloxane substrates are washed with benzene and air-dried in order to remove airborne hydrocarbon contaminants. Benzene is nonpolar, has vapor pressure of 105 Torr at 20 °C,[48] and was found to not stay on the surface following evaporation, as confirmed by the absence of aromatic C−H stretches between 3025 and 3070 cm^{-1}.[49,50] BBSFG spectra showing a hydrolyzed methyl ester-functionalized surface before and after successive benzene rinses are presented in Figure 10. The SFG spectrum of the acid-functionalized siloxane-terminated surface after multiple benzene rinses is reproducible and shown at the bottom of Figure 10. Because the acid has only CH_2 groups, giving rise to two SFG peaks (symmetric and asymmetric CH_2 stretches), the presence of additional peaks, especially from CH_3 symmetric stretches, as indicated by the dashed line at 2880 cm^{-1}, are indicative of hydrocarbon contaminants on the surface. Wang et al. recently reported that such hydrocarbon surface contaminants can play a significant role in the photochemistry of TiO_2.[46] Similar hydrocarbon contamination was also found by Paszti et al.,[51] who studied the interaction of proteins with titanium surfaces. The remarkable differences in the four spectra shown in Figure 10 demonstrate the potential difficulties in the characterization of organic adsorbates. Despite the care taken during synthesis of substrates, organic compounds present in the air can adsorb to samples and can contribute significant amounts of spectral information. Therefore, careful cleaning procedures are necessary to ensure SFG spectra that are free of contributions from organic contaminants.

IV. Conclusions

Using siloxane chemistry, we have functionalized glass substrates with organosilanes that contain terminal carboxylic acid and ester linker groups. Our work uses BBSFG to characterize these functionalized siloxanes on glass, extending the scope of SFG work on functionalized silica substrates, which, until now, had been limited to purely hydrocarbon systems. The distinctive differences in the BBSFG spectra of our samples illustrate the high sensitivity of nonlinear optical spectroscopy in the detection of various end groups, differentiating between samples terminated with different esters, a carboxylic acid, as well as deuterated and fluorinated terminal groups.

The facile attachment chemistry and versatile synthetic modifiability of siloxane scaffolds allow for their use as chemical linkers. Due to the presence of a strong silicon−carbon bond, the tris(alkoxy)silane scaffolds under investigation in this work are chemically robust and allow for further manipulation/modification of the surfaces. In related work, we studied how carboxylic acid- and ester-functionalized siloxanes on fused silica interact with chromium(VI).[35] We also characterized the interfacial acid−base properties of the acid-functionalized siloxanes at the fused silica/water interface[52] using the "χ^3 method" developed by Eisenthal and co-workers.[53] Through the utilization of the reactivity of the terminal carboxylic acid or the ester groups in the tris(alkoxy)silane scaffolds, a wide variety of inorganic and organic molecules can be tethered to fused silica surfaces, which allows for an improved understanding of heterogeneous processes in environmental chemistry, biological systems, or materials science applications.

Acknowledgment. Support for this project is provided by an NSF Career Award (NSF CHE-0348873), the ACS Petroleum Research Fund (Grant 38960-G5S), the Northwestern Institute for Environmental Catalysis (CHE-9810378 and DE-FG02-03-ER15457), the Northwestern Nanoscale Science and Engineering Center (EEC-0118025), a NASA Graduate Student Fellowship in Earth System Science for A.B.V. (NGT-530456), and Shell Oil Company. We gratefully acknowledge donations by Spectra Physics and CVI Laser LLC, fruitful discussion with Professor Karl Scheidt (Northwestern University) and Professor Zhan Chen (University of Michigan), and helpful comments by one of the anonymous reviewers.

References and Notes

(1) Lahann, J.; Mitragotri, S.; Tran, T.-N.; Kaido, H.; Sundaram, J.; Choi, I. S.; Hoffer, S.; Somorjai, G.; Langer, R. *Science* **2003**, *299*, 371.
(2) Zhou, D. J.; Wang, X. Z.; Birch, L.; Rayment, T.; Abell, C. *Langmuir* **2003**, *19*, 10557.
(3) Burke, B. J.; Moad, A. J.; Polizzi, M. A.; Simpson, G. J. *J. Am. Chem. Soc.* **2003**, *125*, 9111.
(4) Chance, J. J.; Purdy, W. C. *Langmuir* **1997**, *13*, 4487.
(5) Hu, K.; Bard, A. J. *Langmuir* **1997**, *13*, 5114.
(6) Ulman, A. *Chem. Rev.* **1996**, *96*, 1533.
(7) Ikeura, Y.; Karihara, K.; Kunitake, T. *J. Am. Chem. Soc.* **1991**, *113*, 7342.
(8) Abbatt, J. P. D. *Chem. Rev.* **2003**, *103*, 4783.
(9) Prime, K. J.; Whitesides, G. M. *Science* **1991**, *252*, 1164.
(10) Plueddemann, E. P. *Silane Coupling Agents*; Plenum Press: New York, 1982.
(11) Zhu, X. D.; Suhr, H.; Shen, Y. R. *Phys. Rev. B: Condens. Matter Mater. Phys.* **1987**, *35*, 3047.
(12) Richmond, G. L. *Chem. Rev.* **2002**, *102*, 2693.
(13) Shen, Y. R. *Nature* **1989**, *337*, 519.
(14) Liu, Y.; Wolf, L. K.; Messmer, M. C. *Langmuir* **2001**, *17*, 4329.
(15) Chen, C.; Loch, C. L.; Wang, K.; Chen, Z. *J. Phys. Chem. B* **2003**, *107*, 10440.
(16) Nihongyanagi, S.; Miyamoto, D.; OIdojiri, S.; Uosaki, K. *J. Am. Chem. Soc.* **2004**, *126*, 7037.
(17) Elmore, D. L.; Leverette, C. L.; Chase, D. B.; Kalambur, A. T.; Liu, Y.; Rabolt, J. F. *Langmuir* **2003**, *19*, 3519.
(18) Snyder, R. G.; Srauss, H. L.; Eilliger, C. A. *J. Phys. Chem.* **1982**, *86*, 5145.
(19) Snyder, R. G.; Hsu, S. L.; Krim, S. *Spectrochim. Acta, Part A* **1978**, *34A*, 395.
(20) Miranda, P. B.; Shen, Y. R. *J. Phys. Chem. B* **1999**, *103*, 3292.
(21) Eisenthal, K. B. *Chem. Rev.* **1996**, *96*, 1343.
(22) Shen, Y. R. *The Principles of Nonlinear Optics*; John Wiley & Sons: New York, 1984.
(23) Boyd, R. W. *Nonlinear Optics*; Academic Press: New York, 1992.
(24) Buck, M.; Himmelhaus, M. *J. Vac. Sci. Technol., A* **2001**, *19*, 2717.
(25) Richter, L. J.; Petralli-Mallow, T. P.; Stephenson, J. C. *Opt. Lett.* **1998**, *23*, 1594.
(26) Wei, X.; Hong, S. C.; Lvovsky, A. I.; Held, H.; Shen, Y. R. *J. Phys. Chem. B* **2000**, *104*, 3349.
(27) Watry, M. R.; Brown, M. G.; Richmond, G. L. *Appl. Spectrosc.* **2001**, *55*, 321A.
(28) Esenturk, O.; Walker, R. A. *J. Phys. Chem. B* **2004**, *108*, 10631.
(29) Hommel, E. L.; Ma, G.; Allen, H. C. *Anal. Sci.* **2001**, *17*, 1325.
(30) Allen, H. C.; Gragson, D. E.; Richmond, G. L. *J. Phys. Chem. B* **1999**, *103*, 660.
(31) Wang, J.; Woodcock, S. E.; Buck, S. M.; Chen, C.; Chen, Z. *J. Am. Chem. Soc.* **2001**, *123*, 9470.
(32) Wang, J.; Chen, C.; Buck, S. N.; Chen, Z. *J. Phys. Chem. B* **2001**, *105*, 12118.
(33) Pangborn, A. B.; Giardello, M. A.; Grubbs, R. H.; Rosen, R. K.; Timmers, F. J. *Organometallics* **1996**, *15*, 1518.
(34) Fryxell, G. E.; Rieke, P. C.; Wood, L. L.; Engelhard, M. H.; Williford, R. E.; Graff, G. L.; Campbell, A. A.; Wiacek, R. J.; Lee, L. F.; Halverson, A. *Langmuir* **1996**, *12*, 5064.
(35) Al-Abadleh, H. A.; Voges, A. B.; Bertin, P. A.; Nguyen, S. T.; Geiger, F. M. *J. Am. Chem. Soc.* **2004**, *124*, 11126.
(36) Noel, O.; Brogly, M.; Castelein, G.; Schultz, J. *Langmuir* **2004**, *20*, 2707.
(37) Gershevitz, O.; Sukenik, C. N. *J. Am. Chem. Soc.* **2004**, *126*, 482.
(38) Chen, C. Y.; Even, M. A.; Wang, J.; Chen, Z. *Macromolecules* **2002**, *35*, 9130.
(39) Opdahl, A.; Phillips, R. A.; Somorjai, G. A. *J. Phys. Chem. B* **2002**, *106*, 5212.
(40) Conboy, J. C.; Messmer, M. C.; Richmond, G. L. *J. Phys. Chem. B* **1997**, *101*, 6724.
(41) Conboy, J. C.; Messmer, M. C.; Richmond, G. L. *Langmuir* **1998**, *14*, 6722.
(42) Guyot-Sionnest, P.; Hunt, J. H.; Shen, Y. R. *Phys. Rev. Lett.* **1987**, *59*, 1597.
(43) Hines, M. A.; Todd, J. A.; Guyot-Sionnest, P. *Langmuir* **1995**, *11*, 493.
(44) Lagutchev, A. S.; Song, K. J.; Huang, J. Y.; Yang, P. K.; Chuang, T. J. *Chem. Phys.* **1998**, *226*, 337.
(45) Himmelhaus, N.; Eisert, F.; Buck, M.; Grunze, M. *J. Phys. Chem. B* **2000**, *104*, 576.
(46) Wang, C.-Y.; Groenzin, H.; Shultz, M. J. *Langmuir* **2003**, *19*, 7330.
(47) Wang, C. Y.; Groenzin, H.; Shultz, M. J. *J. Phys. Chem. B* **2004**, *108*, 265.
(48) *CRC Handbook of Chemistry and Physics*, 71st ed.; CRC Press: Boston, 1990−1991.
(49) Hommel, E. L.; Allen, H. C. *J. Phys. Chem. B* **2003**, *107*, 10823.
(50) Zhang, D.; Dougal, S. M.; Yeganeh, M. S. *Langmuir* **2000**, *16*, 4528.
(51) Paszti, Z.; Wang, J.; Clarke, M. L.; Chen, Z. *J. Phys. Chem. B* **2004**, *108*, 7779.
(52) Konek, C. T.; Musorrafiti, M. J.; Al-Abadleh, H. A.; Bertin, P. A.; Nguyen, S. T.; Geiger, F. M. *J. Am. Chem. Soc.* **2004**, *126*, 11754.
(53) Ong, S.; Zhao, X.; Eisenthal, K. B. *Chem. Phys. Lett.* **1992**, *191*, 327.